Hindawi
Journal of Sensors
Volume 2019, Article ID 5704614, 7 pages
https://doi.org/10.1155/2019/5704614

Research Article

Miniature All-Silica Microbubble-Based Fiber Optic Fabry-Perot Pressure Sensor with Pressure Leading-In Tube

Huixin Zhang, Jia Liu, Jiashun Li, Pinggang Jia, Fei Feng, Yingping Hong, Sanmin Shen, Ting Liang, and Jijun Xiong

Science and Technology on Electronic Test and Measurement Laboratory, North University of China, Taiyuan 030051, China

Correspondence should be addressed to Pinggang Jia; pgjia@nuc.edu.cn

Received 27 September 2018; Revised 24 December 2018; Accepted 20 January 2019; Published 3 April 2019

Academic Editor: Carlos Ruiz

A novel all-silica fiber optic Fabry-Perot (FP) pressure sensor with pressure leading-in tube based on microbubble structure is developed and experimentally demonstrated. The FP cavity is formed by fixing the end face of the single-mode fiber (SMF) parallel to the outer surface of the microbubble, in which the microbubble with a diameter of about 318 μm is constructed at the end of silica hollow tube. When external pressure is transmitted on the inner surface of the microbubble by the pressure leading-in tube, the FP cavity length changes with the diameter of microbubble. Experimental results show that such a sensor has a linear sensitivity of approximately 4.84 nm/MPa at room temperature over the pressure range of 1.1 MPa; the sensor has a very low temperature coefficient of approximately 2 pm/°C from room temperature to 600°C. The sensor has advantages of extremely low temperature coefficient, compact structure, and small size, which has potential applications for measuring pressure in high-temperature environment.

1. Introduction

Fiber optic Fabry-Perot (FP) sensors have been widely studied for measuring pressure, temperature, strain, vibration, ultrasound, etc. because they have the advantages of simple configuration, rapid response, low cost, and immunity to electromagnetic interference [1–7]. In particular, Fabry-Perot sensors for pressure measurement have significant advantages in many areas such as biomedical, downhole oil/gas exploration [7].

Recently, the miniature all-silica fiber optic FP sensors based on microcavity or microbubble have attracted much interest [8–16]. Ma et al. [17] fabricated a compact FP pressure sensor based on a single-mode fiber (SMF) tip microcavity for high-pressure measurement. The sensor is made by fusing a silica capillary to the end of a SMF, tapering the capillary with internal gas pressure, and then melting the capillary at the waist to form an air cavity. The pressure sensitivity is about 147.37 pm/MPa. Liao et al. [18] also demonstrated a submicron silica diaphragm-based fiber tip FP interferometer for pressure measurement by using an improved electrical arc discharge technique. The pressure sensitivity is about 1036 pm/MPa. In addition, Zhao et al. [19] presented a small in-fiber Fabry-Perot low-frequency acoustic pressure sensor with PDMS diaphragm embedded in hollow-core fiber, which achieved a high sensitivity of 0.427 mV/MPa with a high linear pressure response in the range of 5 MPa–720 MPa. Meanwhile, two high-sensitivity strain sensors based on air microbubble were proposed [20]. Liu et al. [21] demonstrated an ultrahigh-sensitivity (12.22 nm/kPa) gas pressure sensor based on the Fabry-Perot interferometer employing a fiber tip diaphragm-sealed cavity; the sensor functions well up to a temperature of about 1000°C. And Liu et al. [22] proposed a strain force sensor based on fiber inline Fabry-Perot microcavity plugged by cantilever taper; the sensor exhibited high strain force sensitivity. In our previous work, a fiber optic FP pressure sensor with low temperature coefficient based on a microbubble is proposed; the sensitivity is about 6.382 nm/MPa [23].

In this letter, a novel all-silica fiber optic Fabry-Perot (FP) pressure sensor with pressure leading-in tube based on microbubble structure is developed and experimentally

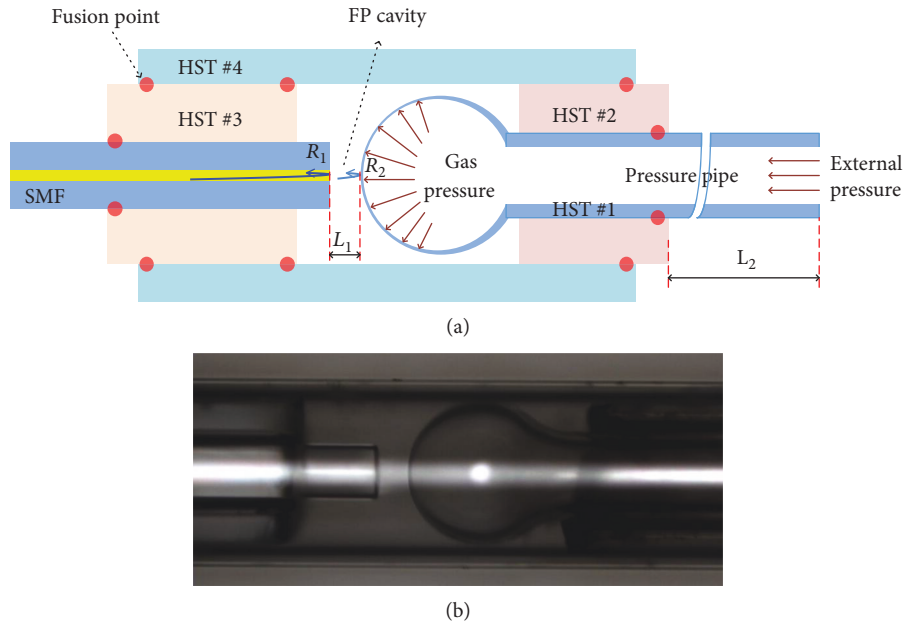

Figure 1: The all-silica microbubble-based fiber optic FP pressure sensor. (a) Structural configuration and (b) photograph.

demonstrated. The FP cavity is formed by fixing the end face of the SMF parallel to the outer surface of the microbubble. When pressure is applied on the inner surface of the microbubble by the pressure leading-in tube, the deflection of the diaphragm of the microbubble will cause the change of FP cavity. On these bases, the fiber optic FP pressure sensor system and the experimental setup are established, and the sensing characteristics of the sensor are tested and analyzed. Due to the all-silica structure, the proposed microbubble-based fiber optic FP pressure sensor has a very low temperature coefficient.

2. Operating Principle

The structural configuration and microphotograph of the proposed microbubble-based fiber optic FP pressure sensor are shown in Figures 1(a) and 1(b), respectively. The sensor mainly consists of a SMF and pressure leading-in tube, and the FP cavity is constructed of four kinds of hollow silica tubes (HSTs) with different diameters. The parameters of HSTs are shown in Table 1. From Figure 1, the FP cavity with the distance of L_1 is formed by placing the end face of the SMF parallel to the outer surface of the microbubble, and the diameter of the microbubble is about 318 μm. The HST #1 with the length of L_2 is used as pressure leading-in tube. When external pressure is transmitted on the inner surface of the microbubble by the pressure leading-in tube (HST #1), the FP cavity length changes with the diameter of the microbubble. Therefore, the external pressure changes can be detected by demodulating the FP cavity length of the sensor.

According to Figure 1, the lights are reflected and refracted between the facets of the SMF and the outer surface of the microbubble; the multibeam interference occurs when the light is reflected into the SMF. As the reflectivity of each glass-air interface is very low (less than 4%), this microbubble-based pressure sensor can be considered as a two-beam interferometer. The reflected light intensity can be expressed as

$$\mathrm{I} = I_1 + I_2 - 2\sqrt{I_1 I_2}\cos\frac{4\pi n_a}{\lambda}L_1, \tag{1}$$

where I_1 and I_2 are the optical intensities of the two reflected lights, n_a is the refractive index of air, L_1 is the length of the FP cavity, and λ is the wavelength of light.

When the external pressure is transmitted on the inner surface of the microbubble, the thin shell of the microbubble could be approximated as an open hemispherical shell with tangential edge support. The length change of the FP cavity of the fiber optic pressure sensor can be written by [20]

$$\Delta L = \frac{r^2(1-\nu)}{2Eh}P, \tag{2}$$

where ΔL is the deflection, P is the pressure applied on the shell, E is the Young modulus, ν is the Poisson ratio, and r and h are the effective radius and thickness of the microbubble, respectively.

According to equation (2), the pressure sensitivity of the fiber optic FP pressure sensor is closely related to the structural parameters of the microbubble. The pressure sensitivity as functions of the radius (r) and the thickness (h) of the microbubble defined by equation (2) is shown in Figures 2(a) and 2(b), respectively. According to Figures 2(a) and 2(b), the pressure sensitivity of the fiber optic FP pressure sensor is proportional to the square of the radius of microbubble and inversely proportional to the thickness of the microbubble. Therefore, we can obtain the larger pressure sensitivity by enlarging the radius of the microbubble and reducing the thickness of the microbubble.

Table 1: The parameters of HSTs used in the sensor.

Part name	Type	Inner diameters (μm)	Outer diameters (μm)
HST #1	YN126200, Yongnian Ruipu Chromatogram Equipment Co. Ltd.	126	200
HST #2	YN205340, Yongnian Ruipu Chromatogram Equipment Co. Ltd.	205	340
HST #3	YN130340, Yongnian Ruipu Chromatogram Equipment Co. Ltd.	130	340
HST #4	YN345450, Yongnian Ruipu Chromatogram Equipment Co. Ltd.	345	450

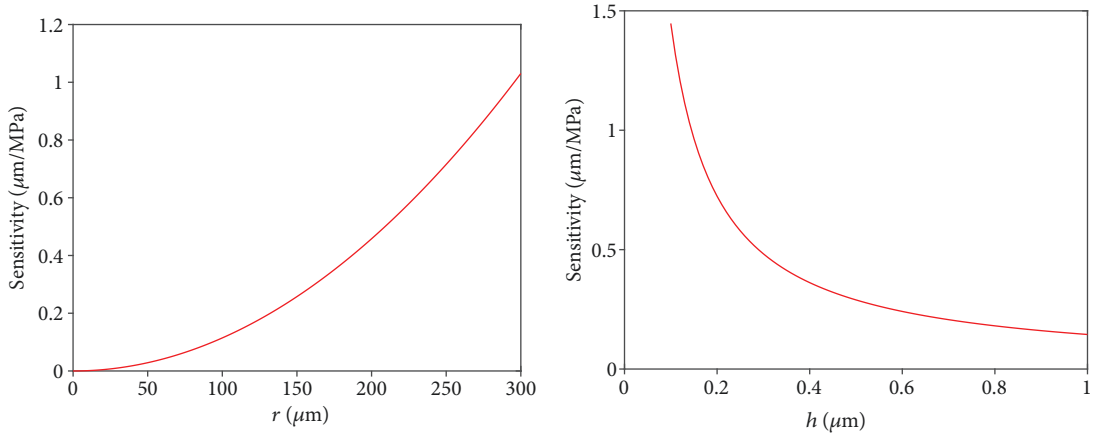

Figure 2: The pressure sensitivity as functions of the structural parameters of microbubble. (a) The radius (r) and (b) the thickness (h) of the microbubble.

3. Sensor Fabrication

Figure 3 shows the fabrication process of the microbubble-based fiber optic Fabry-Perot pressure sensor. From Figure 3, it can be seen that the fabrication process includes five steps. In step 1, as shown in Figure 3(a), the polyimide coating of HST #1 was removed at one end, and the well-cut HST #1 used as pressure leading-in tube was inserted into HST #2. Then, we fused two HSTs together. The length of the pressure leading-in tube can reach several meters. The used parameters of the fusion splicer were (FITEL, S183 version 2, Japan) set as "A" in Table 2. In step 2, as shown in Figure 3(b), the HST #1 was fused at one end by using the manual program of the fusion splicer. The parameters of the fusion splicer about this step were set as "B" in Table 2. In step 3, as shown in Figure 3(c), the other end of the HST #1 was connected to a pneumatic pump (Const 162, China) to allow air pressure to enter in. Meanwhile, the arc discharge was implemented at the fusion end of the HST #1. Due to the slight higher pressure, the end of the HST #1 thermally expanded into a microbubble. During this step, the fusion position could be adjusted by moving the motor and the arc discharge was operated to thin the microbubble wall. The diameter of the microbubble can reach several hundred micrometers by controlling the gas pressure. The parameters of the fusion splicer were set as "C" in Table 2 during the arc discharge. In step 4, as shown in Figure 3(d), a well-cut SMF was inserted into the HST #3. Then, we tightly welded SMF and HST #3 together to achieve seal. The parameters of the fusion splicer were set as "D" in Table 2. In step 5, as shown in Figure 3(e), these two mentioned HST #3 fused with SMF and HST #2 fused with microbubble were inserted into the same well-cut HST #4 from opposite directions. During this step, the parameters of the fusion splicer were set as "E" in Table 2. In the fabrication process, only arc discharge technology is chosen to fabricate the microbubble-based fiber optic Fabry-Perot pressure sensor.

The distance between the end of the SMF and the outer surface of the microbubble can be adjusted. The interference spectrum of three samples of fiber optic Fabry-Perot pressure sensors can be obtained by the spectrometer during the adjusting process, as shown in Figure 4. It can be seen that the contrasts of the interference spectrum are larger than 7 dBm. The calculated cavity length from the reflection spectrum using the fringe counter method is about 57 μm, 138 μm, and 188 μm, respectively. The air cavity of the fabricated fiber optic Fabry-Perot pressure sensor can be seen as a low finesse FP interferometer. The small fluctuation of interference spectrum is mainly caused by the nonparallelity of the end of SMF and the spherical surface of the microbubble. The contrast of the interference spectrum could be improved by optimizing the parameters of the arc discharge.

4. Experiments and Results

Figure 5 shows the schematic diaphragm of the pressure test setup, respectively. It mainly consists of a personal computer (PC), pneumatic pump (Const 162, China), calibrated digital pressure gauge, and optical sensing interrogator (sm125, Micron Optics, America). The end of the pressure leading-in tube (HST #1) of the fiber optic FP pressure sensor is connected to the pneumatic pump. The calibrated digital

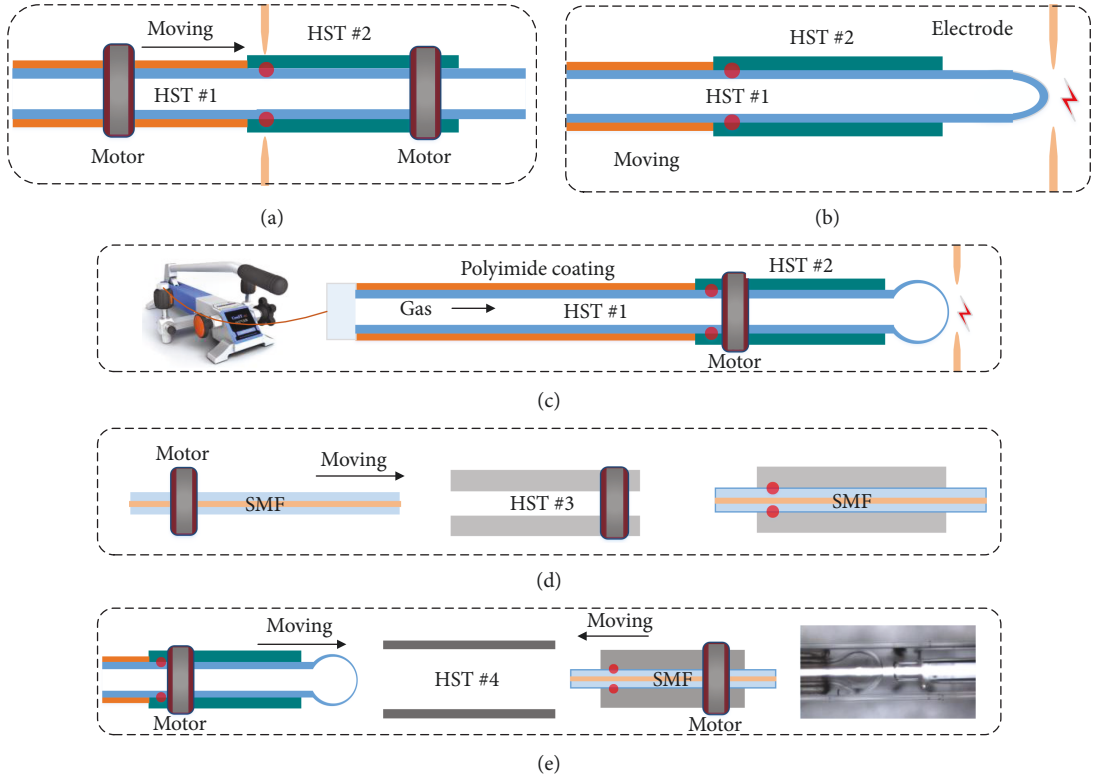

Figure 3: Fabrication process of the microbubble fiber optic Fabry-Perot pressure sensor. (a) Inserting and fusing the HST #1 into HST #2; (b) fusing the one end of the well-cut HST #1; (c) fabricating a microbubble at the end of well-cut HST #1; (d) inserting and fusing the SMF into the HST #3; (e) inserting and fusing HST #2 and HST #3 into the HST #4 from opposite ends.

Table 2: Parameters of the fusion splicer.

	Clean intensity	Clean time	Fusion beginning intensity	Fusion ending intensity	Fusion time	Fusion times
A	200 units	180 ms	100 units	100 units	800 ms	5
B	200 units	200 ms	100 units	100 units	1000 ms	2
C	140 units	100 ms	100 units	60 units	300 ms	4~5
D	200 units	220 ms	120 units	120 units	1000 ms	4~5
E	200 units	250 ms	150 units	150 units	2000 ms	6~8

pressure gauge is also connected to the pneumatic pump to provide pressure reference. The fiber optic FP pressure sensor is connected to the optical sensing interrogator through the fiber optic connector. The light from the optical sensing interrogator propagates to the FP cavity of the sensor along the SMF, and then its interference signal is reflected back to the optical sensing interrogator, and the interference spectrum is displayed in the PC.

During the experiment, the pressure in the pneumatic pump can be manually controlled from atmospheric pressure to 1.1 MPa. Figure 6 shows the reflection spectrum of fiber optic FP pressure sensor with the FP cavity length of 138 μm in a pressure range from almost 0.1 to 1.1 MPa at room temperature. It can be seen that the interference fringe shifts towards a shorter wavelength. Accordingly, the relationship between the wavelength shifts and the gas pressure at room temperature is investigated when the pressure was

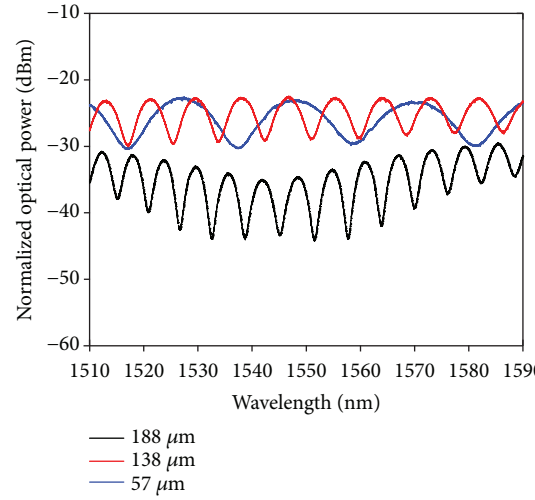

Figure 4: Interference spectrum of the fiber optic FP pressure sensor.

increased and decreased, as shown in Figure 7. It can be seen from Figure 7 that the wavelength shifts are proportional to gas pressure. The sensor shows good repeatability. The average sensitivity of the three tests is approximately 4.84 nm/MPa, and the nonlinearity of the fiber optic FP pressure sensor at room temperature is less than 2.07%.

Figure 8 shows the relationship between the wavelength shifts and temperature of the fiber optic FP pressure sensor when the FP cavity is placed at high temperature. It can be

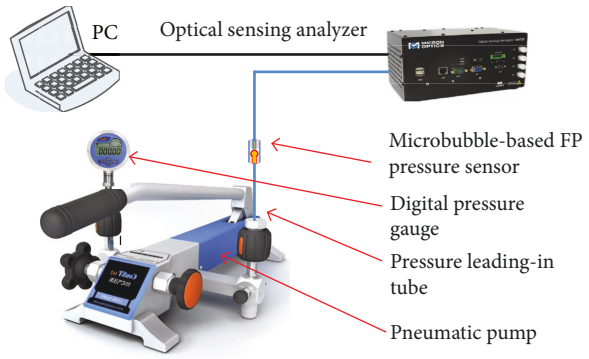

Figure 5: Schematic diagram of the experimental setup for pressure measurement.

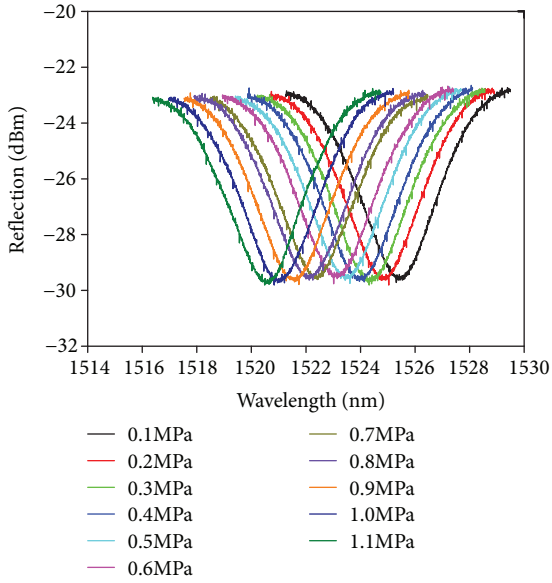

Figure 6: Reflection spectrum of fiber optic FP pressure sensor with pressure range from 0.1 to 1.1 MPa at room temperature.

seen that the FP cavity has the low temperature coefficient of about 2 pm/°C when the operating temperature is lower than 600°C. The low temperature coefficient may be due to the all-silica and temperature-compensated structure. When the operating temperature exceeds 600°C, the temperature coefficient of the sensor is significantly increased, which may be caused by the softening of the silica.

To characterize the stability of the proposed sensor, the wavelength shifts under pressure at 1.1 MPa at room temperature for about 120 minutes were investigated, as shown in Figure 9. It can be seen that the sensor had good stability with slight variations in the wavelength response for at least 120 minutes. The variation is less than 70 pm.

The sensor has potential applications for measuring pressure in high-temperature environment. We can only place the end of the pressure leading-in tube in a high-temperature environment when measuring the pressure. Considering that the hollow silica tubes can survive at high temperature, the proposed microbubble-based fiber optic FP pressure sensor can measure the pressure in the high-

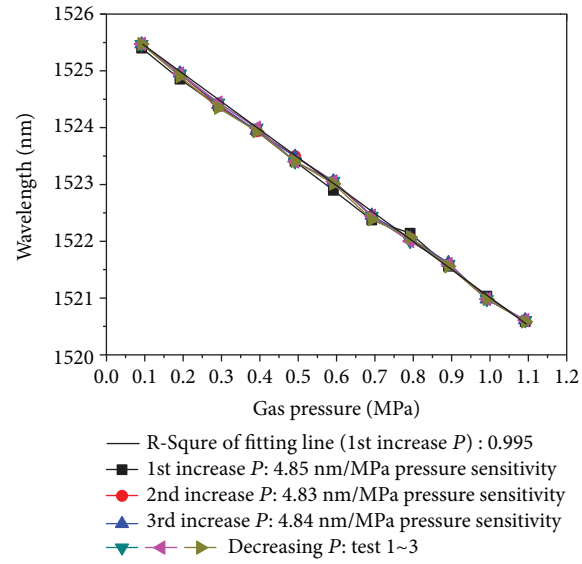

Figure 7: Relationship between the wavelength shifts and the gas pressure at room temperature.

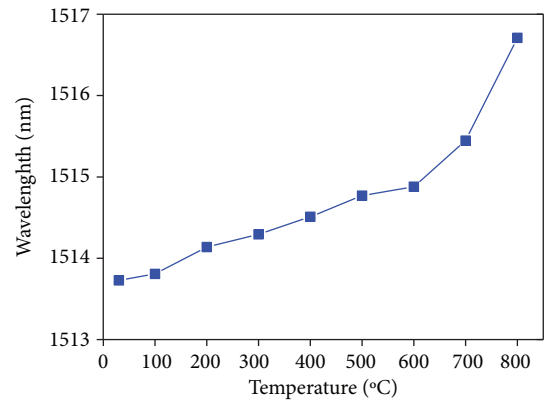

Figure 8: Relationship between the wavelength shifts and temperature of the FP cavity.

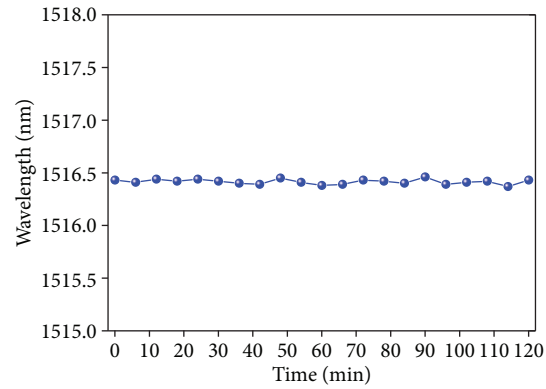

Figure 9: The stability test results of the proposed sensor at 1.1 MPa for 120 minutes.

temperature environment. However, the pressure leading-in tube will affect the dynamic performance of the sensor. The longer the pressure leading-in tube of the sensor, the worse

the dynamic performance is of the sensor. In some cases, a short pressure leading-in tube may be required.

5. Conclusions

A novel all-silica fiber optic FP pressure sensor with a pressure leading-in tube based on microbubble structure is developed and experimentally demonstrated. The FP cavity is formed by fixing the end face of the SMF parallel to the outer surface of the microbubble, in which the microbubble with the diameter of about 318 μm is constructed at the end of the silica hollow tube. Experimental results show that such a sensor has a linear sensitivity of approximately 4.84 nm/MPa at room temperature over the pressure range of 1.1 MPa; the sensor has a very low temperature coefficient of approximately 2 pm/°C from room temperature to 600°C. The sensor has advantages of extremely low temperature coefficient, compact structure, and small size, which has potential applications for measuring pressure in high-temperature environment.

Data Availability

The data used to support the findings of this study are available from the corresponding author upon request.

Conflicts of Interest

The authors declare that there is no conflict of interest regarding the publication of this paper.

Acknowledgments

This work was supported by the National Science Fund for Distinguished Young Scholars under Grant 51425505, the National Natural Science Foundation of China under Grant 51405454, and Fund for Shanxi "1331 Project" Key Subject Construction.

References

[1] Y. Wu, Y. Zhang, J. Wu, and P. Yuan, "Temperature-insensitive fiber optic Fabry-Perot interferometer based on special air cavity for transverse load and strain measurements," *Optics Express*, vol. 25, no. 8, pp. 9443–9448, 2017.

[2] Y. Gong, T. Zhao, Y. J. Rao, and Y. Wu, "All-fiber curvature sensor based on multimode interference," *IEEE Photonics Technology Letters*, vol. 23, no. 11, pp. 679–681, 2011.

[3] H. Yu, Y. Wang, J. Ma, Z. Zheng, Z. Luo, and Y. Zheng, "Fabry-Perot interferometric high-temperature sensing up to 1200°C based on a silica glass photonic crystal fiber," *Sensors*, vol. 18, no. 1, p. 273, 2018.

[4] Z. Chen, S. Xiong, S. Gao et al., "High-temperature sensor based on Fabry-Perot interferometer in microfiber tip," *Sensors*, vol. 18, no. 2, p. 202, 2018.

[5] P. Jia, G. Fang, Z. Li et al., ""Bellows spring-shaped" ultrasensitive fiber-optic Fabry-Perot interferometric strain sensor," *Sensors and Actuators A: Physical*, vol. 277, pp. 85–91, 2018.

[6] H. Liang, P. Jia, J. Liu et al., "Diaphragm-free fiber-optic Fabry-Perot interferometric gas pressure sensor for high temperature application," *Sensors*, vol. 18, no. 4, p. 1011, 2018.

[7] M. R. Islam, M. M. Ali, M. H. Lai, K. S. Lim, and H. Ahmad, "Chronology of Fabry-Perot interferometer fiber-optic sensors and their applications: a review," *Sensors*, vol. 14, no. 4, pp. 7451–7488, 2014.

[8] Y. Zhang, L. Yuan, X. Lan, A. Kaur, J. Huang, and H. Xiao, "High-temperature fiber-optic Fabry–Perot interferometric pressure sensor fabricated by femtosecond laser," *Optics Letters*, vol. 38, no. 22, pp. 4609–4612, 2013.

[9] L. Yan, Z. Gui, G. Wang et al., "A micro bubble structure based Fabry–Perot optical fiber strain sensor with high sensitivity and low-cost characteristics," *Sensors*, vol. 17, no. 3, p. 555, 2017.

[10] Q. Wang, D. Yan, B. Cui, and Z. Guo, "Optimal design of an hourglass in-fiber air Fabry-Perot microcavity-towards spectral characteristics and strain sensing technology," *Sensors*, vol. 17, no. 6, p. 1282, 2017.

[11] Y. Li, W. Zhang, Z. Wang, H. Xu, J. Han, and F. Li, "Low-cost and miniature all-silica Fabry–Perot pressure sensor for intracranial pressure measurement," *Chinese Optics Letters*, vol. 12, no. 11, pp. 111401–111404, 2014.

[12] S. Pevec and D. Donlagic, "Miniature all-fiber Fabry–Perot sensor for simultaneous measurement of pressure and temperature," *Applied Optics*, vol. 51, no. 19, pp. 4536–4541, 2012.

[13] J. Xu, X. Wang, K. L. Cooper, G. R. Pickrell, and A. Wang, "Miniature temperature-insensitive Fabry-Pe/spl acute/rot fiber-optic pressure sensor," *IEEE Photonics Technology Letters*, vol. 18, no. 10, pp. 1134–1136, 2006.

[14] W. Wang, Q. Yu, F. Li, X. Zhou, and X. Jiang, "Temperature-insensitive pressure sensor based on all-fused-silica extrinsic Fabry–Pérot optical fiber interferometer," *IEEE Sensors Journal*, vol. 12, no. 7, pp. 2425–2429, 2012.

[15] X. Zou, N. Wu, Y. Tian et al., "Ultrafast Fabry-Perot fiber-optic pressure sensors for multimedia blast event measurements," *Applied Optics*, vol. 52, no. 6, pp. 1248–1254, 2013.

[16] L. Zi-Liang, L. Chang-Rui, L. Shen, and W. Yi-Ping, "Research progress of in-fiber Fabry-Perot interferometric temperature and pressure sensors," *Acta Physica Sinica*, vol. 66, article 070708, 2017.

[17] J. Ma, J. Ju, L. Jin, and W. Jin, "A compact fiber-tip micro-cavity sensor for high-pressure measurement," *IEEE Photonics Technology Letters*, vol. 23, no. 21, pp. 1561–1563, 2011.

[18] C. Liao, S. Liu, L. Xu et al., "Sub-micron silica diaphragm-based fiber-tip Fabry–Perot interferometer for pressure measurement," *Optics Letters*, vol. 39, no. 10, pp. 2827–2830, 2014.

[19] Y. Zhao, M. Q. Chen, F. Xia, and R. Q. Lv, "Small in-fiber Fabry-Perot low-frequency acoustic pressure sensor with PDMS diaphragm embedded in hollow-core fiber," *Sensors and Actuators A: Physical*, vol. 270, pp. 162–169, 2018.

[20] Y. Zhao, M. Q. Chen, and Y. Peng, "Tapered hollow-core fiber air-microbubble Fabry-Perot interferometer for high sensitivity strain measurement," *Advanced Materials Interfaces*, vol. 5, no. 21, 2018.

[21] S. Liu, Y. Wang, C. Liao et al., "Nano silica diaphragm in-fiber cavity for gas pressure measurement," *Scientific Reports*, vol. 7, no. 1, p. 787, 2017.

[22] Y. Liu, C. Lang, X. Wei, and S. Qu, "Strain force sensor with ultra-high sensitivity based on fiber inline Fabry-Perot micro-cavity plugged by cantilever taper," *Optics Express*, vol. 25, no. 7, pp. 7797–7806, 2017.

[23] Z. Li, P. Jia, G. Fang et al., "Microbubble-based fiber-optic Fabry–Perot pressure sensor for high-temperature application," *Applied Optics*, vol. 57, no. 8, pp. 1738–1743, 2018.